Human Amniotic Fluid Stem Cell Preconditioning Improves Their Regenerative Potential

Cinzia Rota,[1] Barbara Imberti,[1] Michela Pozzobon,[2] Martina Piccoli,[2] Paolo De Coppi,[2,3] Anthony Atala,[4] Elena Gagliardini,[1] Christodoulos Xinaris,[1] Valentina Benedetti,[1] Aline S.C. Fabricio,[5] Elisa Squarcina,[6] Mauro Abbate,[1] Ariela Benigni,[1] Giuseppe Remuzzi,[1,7] and Marina Morigi[1]

Human amniotic fluid stem (hAFS) cells, a novel class of broadly multipotent stem cells that share characteristics of both embryonic and adult stem cells, have been regarded as promising candidate for cell therapy. Taking advantage by the well-established murine model of acute kidney injury (AKI), we studied the proregenerative effect of hAFS cells in immunodeficient mice injected with the nephrotoxic drug cisplatin. Infusion of hAFS cells in cisplatin mice improved renal function and limited tubular damage, although not to control level, and prolonged animal survival. Human AFS cells engrafted injured kidney predominantly in peritubular region without acquiring tubular epithelial markers. Human AFS cells exerted antiapoptotic effect, activated Akt, and stimulated proliferation of tubular cells possibly via local release of factors, including interleukin-6, vascular endothelial growth factor, and stromal cell–derived factor-1, which we documented in vitro to be produced by hAFS cells. The therapeutic potential of hAFS cells was enhanced by cell pretreatment with glial cell line–derived neurotrophic factor (GDNF), which markedly ameliorated renal function and tubular injury by increasing stem cell homing to the tubulointerstitial compartment. By in vitro studies, GDNF increased hAFS cell production of growth factors, motility, and expression of receptors involved in cell homing and survival. These findings indicate that hAFS cells can promote functional recovery and contribute to renal regeneration in AKI mice via local production of mitogenic and prosurvival factors. The effects of hAFS cells can be remarkably enhanced by GDNF preconditioning.

Introduction

NEW APPROACHES FOR the treatment of acute organ injury have led to the recognition of stem cell–based therapy as a potential tool for tissue regeneration [1–8]. The contribution of bone marrow (BM)–derived and cord blood (CB)–derived stem cells to heal and restore renal tissue integrity in response to acute injury has been recently explored [9–16]. Our group has documented that transplanting either murine or human BM-mesenchymal stem cells (hBM-MSCs) in mice with acute kidney injury (AKI) improved tubular injury and ameliorated renal function through local paracrine activity prolonging animal survival [10,14,17]. Finding that MSCs localized in peritubular areas rather than within tubular epithelium implies that stem cells rarely transdifferentiated into renal cells [10,11,14,17]. Renoprotection was also achieved using human CB-MSCs (hCB-MSCs) [15], which further prolonged animal survival as compared with hBM-MSCs. Despite these encouraging results, several issues need to be investigated including the number of cells to be administered to obtain a therapeutic effect, and their purity. Possible restrictions to using hBM and hCB-MSCs may rest on both their limited capacity to grow in culture and difficulties of isolating hCB-MSCs from all samples. Finally, the differentiative capacity of MSCs toward renal phenotype during kidney repair seems to be very confined [11,14,18]. Alternative sources of stem cells with higher plasticity would add value to the employment of cell therapy in terms of supporting tissue regeneration via direct cell replacement.

Embryonic stem cells are the most plastic stem cell population with indefinite self-renewal capacity; however, their employment is limited by ethical and safety issues [19,20]. Similarly, induced pluripotent stem cells still have limitations in regard to their clinical applicability because of high

[1]"Mario Negri" Institute for Pharmacological Research, Centro Anna Maria Astori, Science and Technology Park Kilometro Rosso, Bergamo, Italy.
[2]Stem Cell Processing Laboratory, Clinic of Paediatric Oncohematology, University of Padova, Padova, Italy.
[3]Surgery Unit, Great Ormond Street Hospital and Institute of Child Health, University College London, London, United Kingdom.
[4]Wake Forest Institute of Regenerative Medicine, Wake Forest University of School of Medicine, Winston-Salem, North Carolina.
[5]Department of Clinical Pathology, Regional Center for Biomarkers—ABO Foundation, Venice, Italy.
[6]Istituto Oncologico Veneto (IOV)—IRCCS, Padova, Italy.
[7]Unit of Nephrology and Dialysis, Azienda Ospedaliera Ospedali Riuniti di Bergamo, Bergamo, Italy.

teratogenicity potential [21]. Recently, amniotic fluid has been identified as a new source of stem cells with high plasticity, derived both from extraembryonic structures and embryonic/ fetal tissues after 12 weeks of gestation [22,23]. These cell lines are broadly multipotent with intermediate characteristics between embryonic and adult stem cells. Indeed, human amniotic fluid stem (hAFS) cells, immunoisolated for c-Kit, express embryonic and MSC markers including Oct-4 and SSEA-4, CD29, CD44, CD73, CD90, and CD105 [22]. Human AFS cells can be readily expanded and reach 250 population doubling—characteristics of embryonic cells—while at the same time retaining stable telomerase length and normal karyotype [22]. Clonal hAFS cell lines can differentiate into cells of the 3 embryonic germ layers and possess advantageous behaviors including the feeder independence and nontumorigenicity at late passages, when injected into immunodeficient mice [22]. For all these reasons, hAFS cells with high differentiation potential would be extremely valuable for cell therapy. In an experimental model of naphthalene-induced lung damage, hAFS cells integrate in bronchioalveolar position and differentiate into Clara cells [24]. Long-term experiments, up to 7 months, excluded tumor formation arising from hAFS cells [24]. Murine and hAFS cells displayed strong hematopoietic potential in sublethally irradiated RAG-1–deficient mice [25]. Recently, hAFS cells showed high ability to differentiate into cardiomyocytes in rats with infarcted myocardium [26]. Moreover, green fluorescent protein-transfected hAFS cells were incorporated into primordial kidney structures and expressed the early renal markers ZO-1, glial cell line–derived neurotrophic factor (GDNF), and claudin thus contributing to the development of renal vesicles, C- and S-shaped bodies [27].

Here, we have studied the potential of hAFS cells to regenerate renal tissue and to prolong survival of mice with cisplatin-induced AKI, a setting that closely resembles the clinical condition. Considering the plasticity of hAFS cells, we have investigated whether these cells afford protection through differentiation into renal cells or through local paracrine effects.

Moreover, we evaluated whether preconditioning of hAFS cells with factors able to enhance their migration, engraftment, and survival could maximize the regenerative potential of a stem cell–based therapy.

Materials and Methods

Isolation and culture of human AFS cells

Backup samples of human amniocentesis were collected from consenting volunteer donors, according to guidelines from the Azienda Ospedaliera Padova (protocol number 451P/32887). Cells were expanded or immediately subjected to immunoselection. Human AFS cells were grown in modified α-MEM (Gibco BRL, Gaithersburg, MD) containing 15% ES-FBS (Gibco), 1% glutamine (Gibco), and 1% penicillin/ streptomycin (Gibco), supplemented with 18% Chang B and 2% Chang C (Irvine Scientific, Santa Ana, CA) [22]. The cells were incubated with a mouse monoclonal antibody anti-CD117 (c-Kit; Santa Cruz Biotechnology, Santa Cruz, CA) followed by goat anti-mouse IgG MicroBeads (Dynal; Invitrogen, Carlsbad, CA) and then selected on a DynalBeads apparatus. Human AFS cells were subcultured at a dilution of 1:4 to 1:8 and expanded up to 70% of confluence. All the in

vitro and in vivo experiments were performed with hAFS cells between passages 6 and 8.

Differentiation of human AFS cells (2–7th passage) toward adipocytes and osteocytes was obtained by exposing cells to specific inductive media, as previously described [22]. Oil-Red-O staining (Sigma-Aldrich, St. Luis, MO) and Von Kossa staining (Sigma) were used to assay lipid droplet accumulation and calcium deposition, respectively.

Cytospin and cytofluorimetric analysis of c-kit–positive hAFS cells

Immunofluorescence of hAFS cells after cytospin was performed at first passage. Phenotypic fluorescence activated cell sorter (FACs) analysis of hAFS cells was studied by incubating cells with anti-human antibodies: CD29 FITC, CD44 FITC, CD73 PE, CD90 FITC, CD105 PE, CD80 FITC, and CD86 PE (Beckton Dickinson, Pharmingen, San Jose, CA); Oct-4 FITC and SSEA-4 FITC (Santa Cruz). Cells have been analyzed for HLA-ABC FITC and HLA-DR PE (Immunotech, Marseille, France).

In vivo experiments

Female 2-month-old NOD-SCID mice (Charles River Italia s.p.a., Calco, Italy) were used. Animal care and treatment were conducted in conformity with the institutional guidelines and international laws and policies. Mice received s.c. 15.5 mg/kg cisplatin (Ebewe Italia Srl, Roma, Italy) and after 24 h were divided into two groups receiving an intravenous (IV) injection as follows: group 1, saline ($n=11$); group 2, hAFS cells (5×10^5 cells/mouse) ($n=11$). Mice were sacrificed at 4 days after cisplatin and kidneys were used for histology and immunohistochemistry. Renal function was assessed as blood urea nitrogen (BUN) by the Reflotron test (Roche Diagnostics Corporation, Indianapolis, IN). Moreover, tubular injury was evaluated in cisplatin-treated mice ($n=3$) sacrificed at 24 h, the time at which stem cells were infused. Normal mice served as controls ($n=11$). To assess survival, cisplatin-treated mice given saline ($n=7$) and cisplatin-treated mice infused with hAFS cells (5×10^5 cells/mouse) ($n=9$) were used. The effect of hAFS cell infusion (5×10^5 cells/mouse) on survival of mice with AKI was compared with that of hBM-MSCs (5×10^5 cells/mouse) and saline ($n=6$ animals for each group). The effect of human fibroblasts infused in cisplatin NOD-SCID mice, as control, has been previously reported [14].

In addition, we compared the effect of hAFS cells with that of hAFS cells preconditioned with GDNF (100 ng/mL for 24 h; Abcam, Inc., Cambridge, MA) before injection [28]. Twenty-four hours after cisplatin, mice were divided into three groups and IV injected as follows: group 1, saline ($n=9$); group 2, hAFS cells (5×10^5 cells/mouse) ($n=10$); group 3, GDNF preconditioned hAFS cells (5×10^5 cells/mouse) ($n=10$). Animals were sacrificed at 4 days for BUN determination, renal histology, and immunohistochemistry. Additional groups of control and cisplatin mice ($n=3$ animals) infused with hAFS cells, untreated or treated with GDNF, were sacrificed after 24 h for quantification of cell engraftment.

Renal morphology

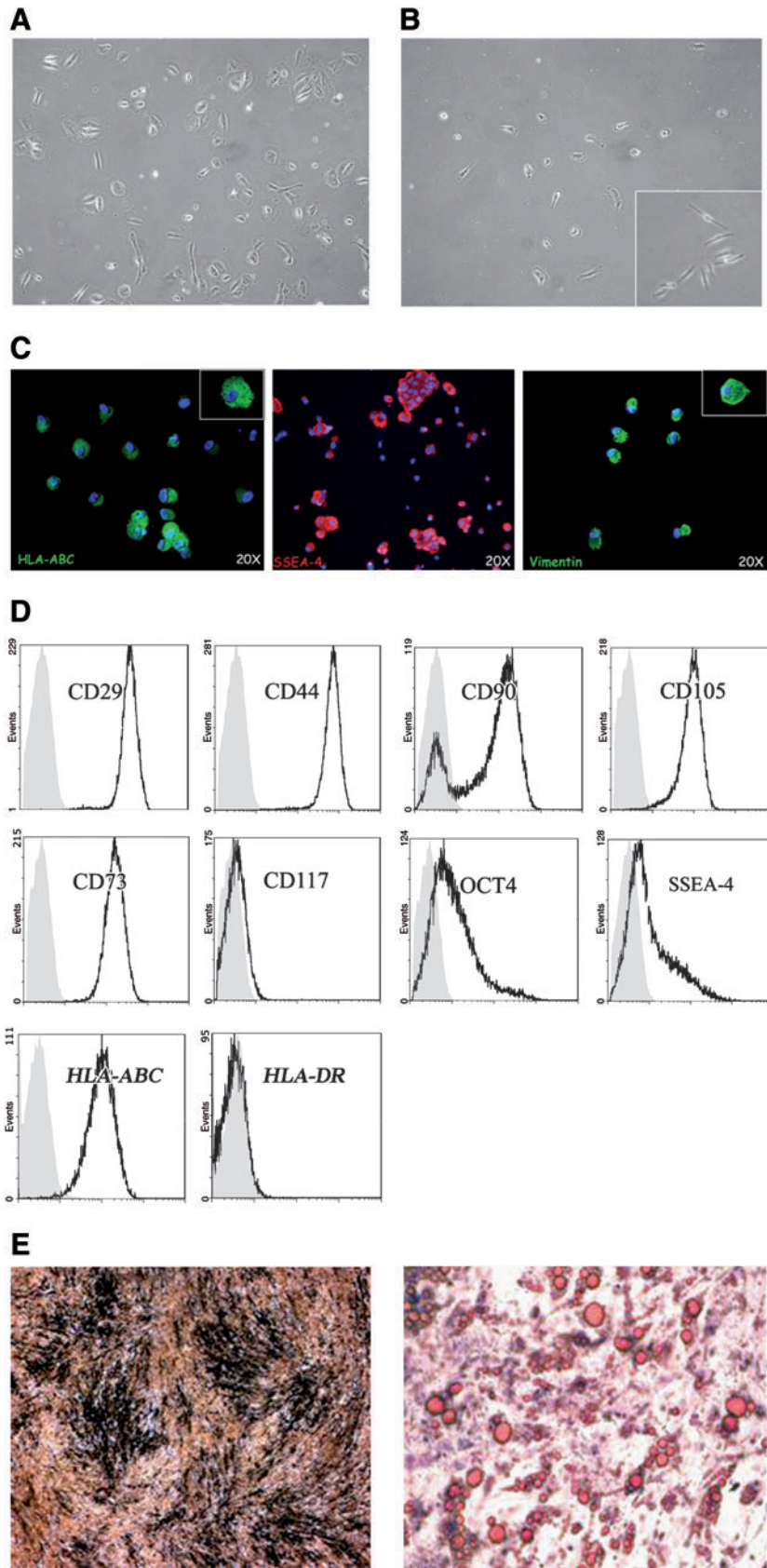*Renal histology.* Kidney samples were fixed in Duboscq-Brazil and paraffin sections were stained with hematoxylin

FIG. 1. Characterization of human AFS cells. (A) Phenotypic appearance of the amniotic sample after amniocentesis: cells show different shape and volume. Original magnification 20×. (B) Human AFS cells after 5 days of selection for c-kit, receptor of the stem cell factor (SCF). Selected cells showed a characteristic morphology: small oval shape that during maturation in culture becomes bigger. Original magnification 20×; inset 40×. (C) Representative images of hAFS cells (first passage) showing positive staining for HLA-ABC, SSEA-4, and vimentin. Magnification 20×. (D) Representative histograms by fluorescence activated cell sorter (FACs) analysis showing the expression of CD29, CD44, CD90, CD105, CD73, CD117, Oct-4, SSEA-4, HLA-ABC, and DR of hAFS cells at 8th passage. The respective isotype control is shown as a *gray* line. (E) Osteogenic differentiation of hAFS cells was evidenced by Von Kossa staining with area of mineralization (*left panel*); adipogenic differentiation of hAFS cells was visualized by Oil-Red-O staining (*right panel*). Original magnification 20×. AFS, amniotic fluid stem. Color images available online at www.liebertonline.com/scd

and eosin, or periodic acid–Schiff's reagent (PAS). Luminal hyaline casts and tubular necrosis (denudation of tubular basement membrane) were assessed in nonoverlapping fields (up to 28 for each section) (40×, high power field, HPF) [15].

Electron microscopy. Fragments of kidney tissue were fixed for 4 h in 2.5% glutaraldehyde in 0.1 M cacodylate buffer, pH 7.4, and washed repeatedly in the same buffer. After postfixation in 1% OsO$_4$, specimens were dehydrated through ascending grades of alcohol and embedded in Epon resin. Ultrathin sections were stained with uranyl acetate and lead citrate and examined using a Philips Morgagni electron microscope.

Quantification of PKH-26–labeled hAFS cells

Human AFS cells, untreated or preconditioned with GDNF, were labeled with PKH-26 red fluorescence cell linker (Sigma-Aldrich, St. Luis, MO) following the manufacturer's instructions and then were infused in control mice or in cisplatin-treated mice. Labeling efficacy was assessed to be >98%. Viability, evaluated by Trypan blue exclusion, was >96%. At different time points, hAFS cell–treated mice were sacrificed and frozen kidney sections were stained with FITC-labeled lectin Wheat Germ Agglutinin (WGA; Vector Laboratories, Burlingame, CA) and 4′,6′-diamidino-2-phenylindole dihydrochloride hydrate (DAPI; Sigma-Aldrich) as previously reported [14]. Ten to twenty sections/mouse (n=3–6 animals for each time point) were analyzed. Data are expressed as number of PKH-26 cells per 10^5 renal cells. The percentage of hAFS cells in tubular and peritubular areas was calculated as number of PKH-26–positive cells in each compartment per total PKH-26 cells. Stem cell engraftment in other organs such as lung, liver, heart, and spleen was also evaluated in control and cisplatin-treated mice (n=3). Nuclei were stained with DAPI.

Immunohistochemistry

Apoptosis. Apoptosis was measured by a terminal transferase-mediated dUTP nick-end labeling (TUNEL) assay (Roche Mannheim, Germany) followed by counterstaining with Rhodamine-labeled lectin Lens Culinaris Agglutinin (LCA; Vector laboratories) and DAPI. Apoptotic nuclei and

TABLE 1. PHENOTYPIC ANALYSIS OF HUMAN AMNIOTIC FLUID STEM ckit+CELLS

Antibody	P4 (%)	P8 (%)
CD29	99.95	82.94
CD44	99.81	82.77
CD90	90.55	77.51
CD105	99.27	90.7
CD73	99.85	95.80
CD117	4.41	2.10
OCT4	69.50	50.50
SSEA-4	38.26	33.21
HLA-ABC	42.50	28.01
HLA-DR	0.58	0.12

Five different cell cultures were analyzed at 4th (P4) and 8th (P8) passages. Standard deviation was ≤10%.

DAPI-positive cells/field (10 fields/mouse; n=3 mice for each group) were counted.

Akt. Frozen kidney sections were fixed in acetone, incubated with anti-phosphorylated (p)Akt (Ser 473) antibody (Cell Signaling Technology, Danvers, MA) followed by goat anti-rabbit-Cy3 (Jakson Immunoresearch). Slides were counterstained with FITC-labeled lectin WGA (Vector Laboratories) and DAPI. Fifteen fields/mouse (n=3 mice for each group) were analyzed and pAkt-positive tubules were counted and expressed as percentage of positive tubules/field.

Proliferation Ki-67. Frozen sections were incubated with mouse anti-Ki-67 antibody (NovoCastra Laboratories) followed by Cy3-conjugated goat anti-mouse antibody (Jackson Immunoresearch). Slides were counterstained with FITC-labeled lectin WGA (Vector Laboratories) and nuclei were visualized by DAPI. Evaluation of Ki-67–positive cells in tubular profiles was performed in at least 10 HPF/section (n=3 mice for each group).

In vitro assays

Wound healing. Confluent hAFS cells were cultured in growth medium for 24 h with or without 100 ng/mL GDNF. Cells were scratched with a 200-µL pipette tip to create an artificial wound and images of wounded monolayer were obtained after 7 h.

Cell viability assay. Human AFS cells were exposed to medium alone or GDNF 100 ng/mL for 24 h and then incubated with H$_2$O$_2$ 200 µM for 24 h. Adherent cells were counted and data were expressed as percentage of viable cells over the total number of untreated control cells (n=3 experiments).

FACs analysis. Human AFS cells treated with or without GDNF 100 ng/mL for 24 h were incubated with mouse anti-CD44 or rabbit anti-CXCR4 (Abcam, Cambridge, UK) or rabbit anti-CX3CR1 (Torrey Pines Biolabs, Inc., East Orange, NJ) antibodies followed by goat anti-mouse or goat anti-rabbit FITC secondary antibodies (Jackson Immunoresearch Laboratories, Inc., West Growe, PA).

Immunofluorescence analysis

To identify the human origin of hAFS cells, frozen kidney sections of mice injected with PKH-26–positive cells were stained with mouse anti-human CD105 antibody (DakoCytomation, Glostrup, Denmark), followed by anti-mouse Cy5 (Jackson Immunoresearch Laboratories, West Baltimore, Pike).

Measurement of cytokine and growth factor production in culture supernatant

Commercially available human multiplex kits (Milliplex MAP; Millipore, Billerica, MA) were used to quantify the production of interleukin (IL)-6 and IL-10, as well as vascular endothelial growth factor (VEGF), fibroblast growth factor 2 (FGF-2), hepatocyte growth factor (HGF), and stromal cell–derived factor-1 (SDF-1α+β), in conditioned media of hAFS cells untreated or treated for 48 h with GDNF 100 ng/mL (n=3 experiments). IGF-1 was measured using Human IGF-I Quantikyne ELISA Kit (R&D Systems, Inc., Minneapolis, MN). IL-6, IL-10, and VEGF were measured using the MILLIPLEX MAP Human Magnetic Cytokine/Chemokine I Panel-3 Plex Kit (Millipore, Billerica, MA). FGF-2, HGF, and
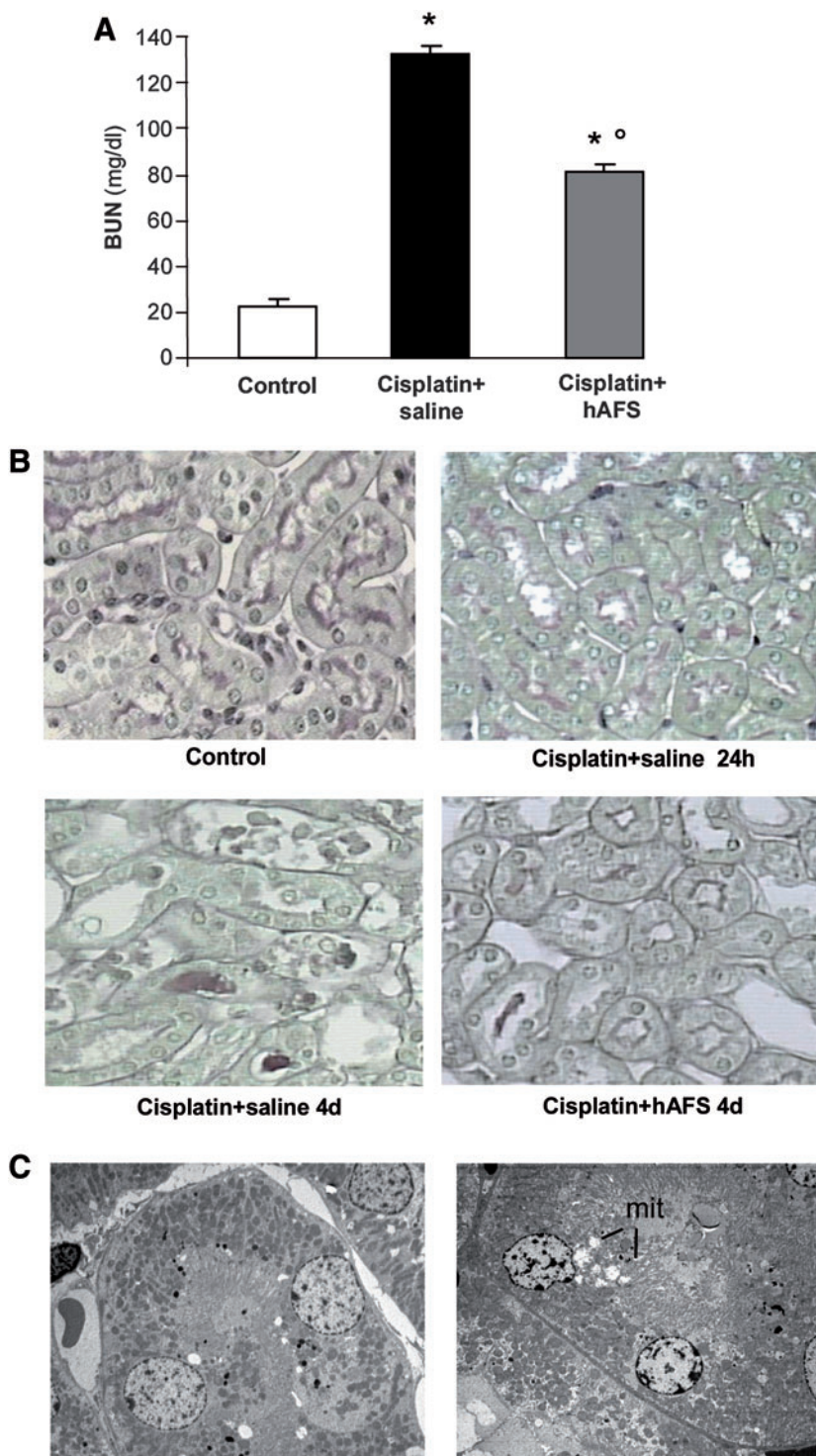
FIG. 2. Human AFS cell infusion protects NOD-SCID mice with AKI from renal function impairment and tubular injury. **(A)** Renal function, assessed as BUN, in control and in cisplatin-treated mice given saline or hAFS cells at 4 days. Data are mean ± SE. *$P < 0.01$ versus control; °$P < 0.01$ versus cisplatin + saline. **(B)** Representative light micrographs of PAS-stained sections of kidneys taken from a control mouse or from mice at 24 h (the time of hAFS cell infusion) or 4 days after cisplatin administration. Casts and necrosis were found at 4 days after cisplatin and were less prominent upon hAFS treatment. Original magnification 400×. **(C)** Electron micrographs of sections of proximal tubuli from a control mouse kidney (*left*) and a 24 h cisplatin-treated mouse (*right*), showing cisplatin-induced mitochondrial swelling (mit) and loss of brush border. Original magnification 2,500×. AKI, acute kidney injury; BUN, blood urea nitrogen; PAS, periodic acid–Schiff's reagent. Color images available online at www.liebertonline.com/scd

SDF-1 were measured using the MILLIPLEX MAP Human Magnetic Circulating Cancer Biomarker Panel-3 Plex Kit (Millipore, Billerica, MA). Multianalyte profiling was performed on the Bioplex 200 Suspension Array System (Bio-Rad, Hercules, CA). All samples were coded for a blinded analysis, and each sample concentration was determined in duplicate. Data were processed with Bio-Plex Manager 5.0 software (Bio-Rad, Hercules, CA). Results were expressed as pg/mL/10^6 hAFS cells. Assay sensitivities (minimum detectable levels + 2 SD) were as follows: IL-6, 0.2 pg/mL; IL-10, 0.5 pg/mL;

VEGF < 5.8 pg/mL; HGF, 6.8 pg/mL; FGF-2, 3.2 pg/mL; SDF1, 33.9 pg/mL; IGF-1, from 7 to 56 pg/mL. The percentage of augmentation of IL-6, VEGF, and SDF-1 production in GDNF-treated over untreated hAFS cells was also calculated as [GDNF/hAFS cells]–[hAFS cells]/[hAFS cells] ×100.

Statistical analysis

Results are expressed as mean ± SE. Statistical analysis was performed using analysis of variance followed by Tukey

TABLE 2. EFFECT OF HUMAN AMNIOTIC FLUID STEM CELLS
ON RENAL HISTOLOGY OF ACUTE KIDNEY INJURY
MICE AT 4 DAYS

	Casts (n/HPF)	Tubular necrosis (n/HPF)
Control	0	0
Cisplatin + saline	8.6 ± 1.2^a	5.2 ± 0.8^a
Cisplatin + hAFS	2.1 ± 0.8^b	2.1 ± 0.8^b

Data are mean ± SE.
[a]$P < 0.01$ versus control.
[b]$P < 0.01$ versus cisplatin + saline.
hAFS cells, human amniotic fluid stem cells; HPF, high-power field; SE, standard error.

Cicchetti test for multiple comparisons or Bonferroni *post hoc* analysis, and unpaired *t*-test using Sigmaplot software, version 11.0 (Systat Software, Inc., Chicago, IL). Nonparametric Kruskal-Wallis test or Kaplan-Meier analysis and Log-Rank test were applied, as appropriate. Statistical significance was defined as $P < 0.05$.

Results

Isolation and characterization of human amniotic fluid stem cells

Human AFS cells were isolated by immunoselection of cells positive to c-kit (CD117) and characterized as previously described [22]. Figure 1A shows hAFS cells immediately after the amniocentesis, where different cell types are present. After c-kit selection (Fig. 1B), the cells presented a small oval shape. Immunofluorescence analysis of hAFS cells, at first passage, showed positivity for HLA-ABC, SSEA4, and vimentin (Fig. 1C).

Phenotypic FACs analysis showed that human AFS cells stably expressed CD29, CD44 (hyaluronate receptor), and stromal cell markers such as CD90 (Thy-1), CD105 (endoglin, TGF-β receptor), and CD73 at 4th and 8th passages (Table 1 and Fig. 1D). The expression of c-kit was progressively lost after passaging (Table 1). The embryonic stem cell markers Oct-4 (POU5f1, POU-domain transcription factor) and SSEA-4 (stem cell embryonic antigen-4) were expressed by hAFS cells after 8 passages of culture (Table 1 and Fig. 1D). Human AFS cells also expressed HLA-ABC but not HLA-DR (Table 1 and Fig. 1D). The absence of HLA-DR indicates low immu-

TABLE 3. QUANTIFICATION OF HUMAN AMNIOTIC FLUID
STEM PKH-26+ CELLS IN RENAL TISSUE OF CISPLATIN MICE

	hAFS cells/10^5 renal cells	% hAFS cells in peritubular areas
hAFS 24 h	2.9 ± 0.2^a	$93\% \pm 4\%$
hAFS 4 days	0.9 ± 0.3	$90\% \pm 7\%$
GDNF/hAFS 24 h	4.9 ± 0.3^b	$90\% \pm 8\%$
GDNF/hAFS 4 days	3.6 ± 0.5^a	$94\% \pm 4\%$

GDNF/hAFS cells, human amniotic fluid stem cells preconditioned for 24 h with GDNF 100 ng/mL. Data are mean ± SE.
[a]$p < 0.01$ versus hAFS 4 days.
[b]$p < 0.05$ versus hAFS 24 h.
GDNF, glial cell line–derived neurotrophic factor.

nogenicity profile. This was further confirmed by absence of detectable CD80 and CD86 (data not shown). Osteogenic and adipogenic differentiation was observed in hAFS cells upon incubation with the appropriate inductive media (Fig. 1 E, right and left panels).

Human AFS cells improve renal function and reduce the severity of renal structural injury

The capability of hAFS cells to exert renoprotective effects was investigated in a mouse model of cisplatin-induced AKI. Immunodeficient NOD-SCID mice injected with cisplatin developed renal function impairment characterized by high serum levels of BUN starting at 3 days (basal, 23.1 ± 1; 24 h, 24.4 ± 1; and 3 days, 98.7 ± 9 mg/dL) that further increased at 4 days (133 ± 4 mg/dL) (Fig. 2A). A significant decrease ($P < 0.01$) of BUN levels at 4 days was observed following hAFS cell injection as compared with cisplatin-treated mice given saline (Fig. 2A).

No structural changes were found in kidneys by light microscopy at 24 h after cisplatin injection, the time of hAFS cell administration (Fig. 2B). Ultrastructural analysis showed focal changes consisting of swelling of mitochondria, loss of brush border, and myelin figures in tubular epithelial cells (Fig. 2C), as previously described [14]. At 4 days, renal histology showed focal and severe tubular cell degenerative alterations (Table 2 and Fig. 2B) including nuclear fragmentation and loss of tubular epithelium. Hyaline casts were prominent. The majority of the injured tubules exhibited areas of necrosis (Table 2 and Fig. 2B). Human AFS cells markedly attenuated renal tubular damage, as reflected by the significant reduction ($P < 0.01$) of necrotic tubules and casts (Table 2 and Fig. 2B).

Human AFS cell distribution in renal and nonrenal tissues

The ability of hAFS cells to engraft the renal parenchyma of cisplatin-treated mice was assessed by labeling stem cells with PKH-26. As shown in Table 3, the frequency of hAFS PKH-26 cells in the injured renal tissue 24 h after their infusion averaged 2.9 ± 0.2 cells/10^5 renal cells and declined during time as assessed at 4 and 31 days (0.9 ± 0.3 and 0.2 ± 0.2 PKH-26 + cells/10^5 renal cells, respectively). At all the time points studied, PKH-26–positive hAFS cells were localized predominantly in peritubular areas (Table 3 and Fig. 3A) and rarely found within tubular epithelium. The human origin of PKH-26–labeled hAFS cells was confirmed in kidney sections costained with anti-human CD105 antibody (Fig. 3B). Immunofluorescence studies indicated that hAFS cells did not acquire tubular markers including cytokeratin and aquaporin-1 at 31 days (data not shown).

The engraftment of human AFS cells in cisplatin mice was also evaluated in liver, heart, spleen, and lung at different times. As shown in Table 4, we have been unable to find at 24 h, hAFS cells in organs other than kidney. At 4 days, no hAFS cells were detected in liver, heart, and spleen, while few PKH-26–positive cells were found in the lung (Table 4).

In control animals infused with hAFS cells, no engraftment was observed in the kidney and in the other organs at 24 h.
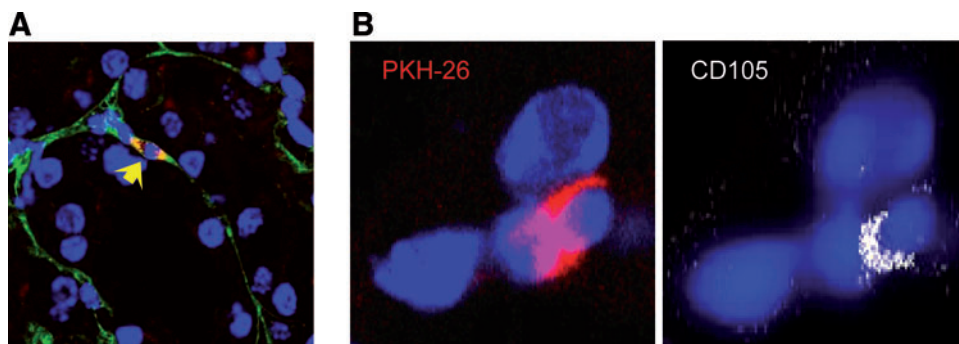
FIG. 3. Human AFS cells engraft the kidney in cisplatin mice. **(A)** Representative micrograph of kidney tissue from cisplatin-treated mouse injected with PKH-26–labeled hAFS cells (*red*) at 4 days. Human AFS PKH-26 + cells were localized in peritubular area (*arrow*). Original magnification 630×. The sections were stained with FITC-labeled lectin WGA (*green*), and DAPI for nuclei (*blue*). **(B)** Representative images of hAFS cells costained with PKH-26 (*left, red*) and human antigen CD105 (*right, white*). Nuclei were stained with DAPI (*blue*). Original magnification 630×. WGA, wheat germ agglutinin; DAPI, 4′,6′-diamidino-2-phenylindole dihydrochloride hydrate. Color images available online at www.liebertonline.com/scd

Human AFS cell treatment inhibits apoptosis, induces Akt phosphorylation, and proliferation of renal tubular cells

Cell apoptosis is one of the major determinants of tubular cell loss both in in vitro and in vivo models of cisplatin-induced toxicity [29]. Mice with cisplatin-induced AKI at 4 days exhibited high (*P* < 0.01) numbers of apoptotic TUNEL-positive cells in damaged tubuli (Fig. 4A, B). Infusion of hAFS cells led to a significant (*P* < 0.01) decrease of TUNEL-labeled cells in respect to cisplatin mice given saline (Fig. 4A, B), indicating their anti-apoptotic activity.

The ability of hAFS cells to activate the serine-threonine kinase Akt, a mediator of survival signals known to counteract apoptosis and to activate mitogenic pathways [30,31], was investigated. In mice with AKI, the expression of phosphorylated Akt (p-Akt) at tubular level declined at 4 days with respect to control animals (Fig. 4C, D), and the treatment with hAFS cells significantly (*P* < 0.01) increased the number of tubules positive for p-Akt (Fig. 4C, D).

The effect of hAFS cell administration on tubular cell proliferation, as an index of renal regeneration, was investigated by assessing the number of tubular epithelial cells positive for Ki-67, a nuclear marker of cycling cells. As
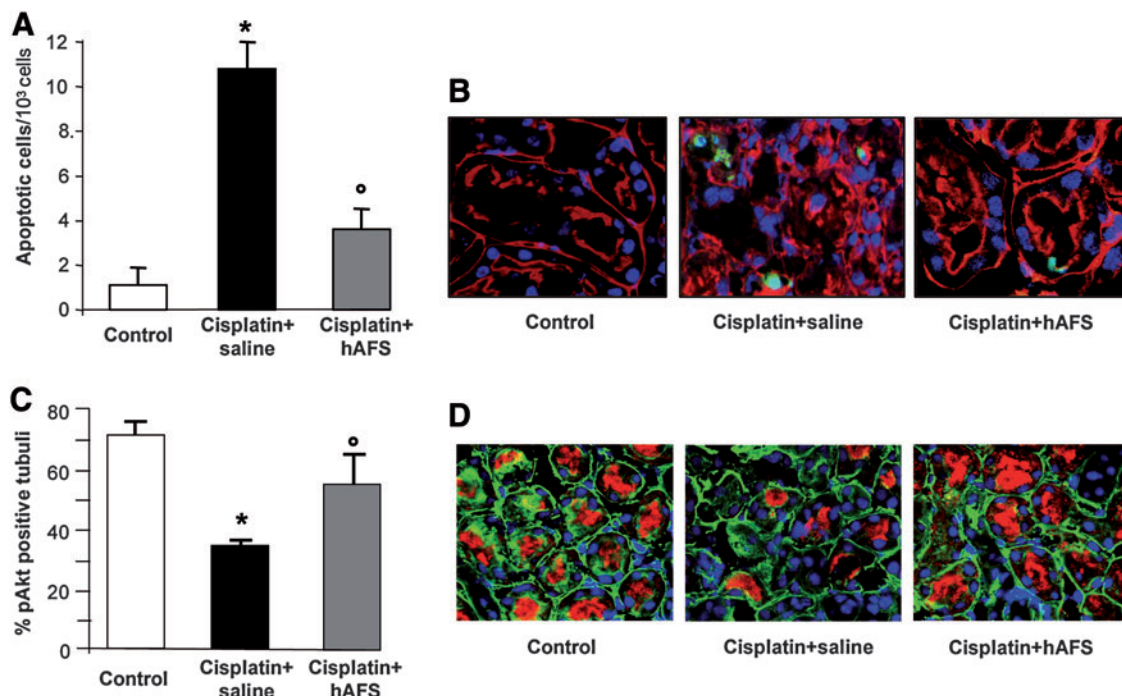

FIG. 4. Human AFS cell treatment reduces apoptosis, and enhances Akt phosphorylation in mice with AKI at 4 days. **(A)** TUNEL-positive cells quantified in kidney sections of control mice, cisplatin-treated mice given saline or hAFS cells. **P < 0.01 versus control; °*P* < 0.01 versus cisplatin + saline. **(B)** Representative images of kidney sections labeled with TUNEL (*green*), rhodamine-labeled lectin LCA (*red*), and DAPI (*blue*). Original magnification 630×. **(C)** Percentage of pAkt-positive tubules in control mice, cisplatin-treated mice receiving saline or hAFS cells. **P < 0.01 versus control; °*P* < 0.01 versus cisplatin + saline. **(D)** Representative images of pAkt staining (*red*) with FITC-labeled lectin WGA (*green*) and DAPI (*blue*) in kidney sections of control, cisplatin mice given saline or hAFS cells. Original magnification 630×. Color images available online at www.liebertonline.com/scd

TABLE 4. QUANTIFICATION OF HUMAN AMNIOTIC FLUID
STEM PKH-26+ CELLS IN DIFFERENT ORGANS
OF CISPLATIN MICE WITH ACUTE KIDNEY INJURY

	PKH-26+ cells/10^5 cells			
	Liver	Lung	Heart	Spleen
hAFS 24 h	0	0	0	0
hAFS 4 days	0	0.8±0.1	0	0

Data are mean±SE.

shown in Fig. 6D and E, a marked induction of tubular cell proliferation was observed at 4 days in renal tissue of cisplatin-treated mice in response to hAFS cell injection.

Human AFS cell treatment prolongs survival of mice with AKI

The effect of hAFS cell treatment on survival of cisplatin mice receiving saline or hAFS cells was investigated. As shown in Fig. 5, NOD-SCID mice with AKI were susceptible to the toxic effect of cisplatin and started to die from day 5. All animals receiving saline died within day 7 (Fig. 5) with high BUN levels (≥140 mg/dL). Infusion of hAFS cells significantly ($P < 0.005$) increased the lifespan of mice with AKI to the extent that 100% of animals were alive at 5 days, 56% of animal survived at 7 days, and 33% of animals were still alive at the end of the study at 31 days.

The ability of hAFS cells to prolong animal survival was also compared with that of hBM-MSCs. As shown in Table 5, survival of cisplatin mice treated with hAFS cells or hBM-MSCs was prolonged in respect to mice receiving saline ($P < 0.009$). The effect on animal lifespan observed with hAFS cells and hBM-MSCs was comparable (Table 5).

Preconditioning with GDNF enhances the regenerative potential of hAFS cells

In the attempt to enhance the therapeutic potential of hAFS cell treatment, we tested the effect of hAFS cells preexposed to GDNF, a member of the transforming growth factor family, known to increase stem cell motility and survival in response to oxidative stress [28]. As shown in Table 3, hAFS cells after preconditioning with GDNF for 24 h before their in vivo infusion exhibited an increased capacity to
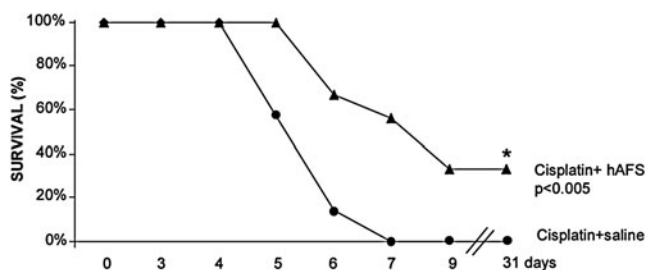

FIG. 5. Human AFS cells improve survival of mice with AKI. Human AFS cell treatment prolongs survival in mice with AKI. At 7 days all mice receiving saline died, while 56% of NOD-SCID mice given hAFS cells survived. *$P < 0.005$ versus cisplatin + saline.

engraft and survive in the damaged renal tissue in respect to untreated hAFS cells. GDNF-treated hAFS cells were predominantly localized in peritubular areas (Table 3 and Fig. 6A, B), similarly to unstimulated cells (Fig. 3A). When infused in control NOD-SCID mice, preconditioned hAFS cells did not migrate in the kidney and in the other organs.

Renal function and tubular alterations were further ameliorated by GDNF-treated hAFS cells as compared with mice receiving untreated cells (Fig. 6B, C). Pretreatment with GDNF markedly enhanced hAFS cell ability to induce tubular cell proliferation (Fig. 6D, E).

GDNF fosters in vitro hAFS cell motility, chemokine/ adhesive receptors, and survival

To identify the mechanisms underlying the renoprotection by GDNF-treated cells in AKI mice, first we tested in vitro whether GDNF incubation for 24 h could enhance hAFS cell motility in a wound healing assay. Human AFS cells treated with GDNF rapidly reduced the surface area of the wound at 7 h in respect to untreated cells (Fig. 7A, B). Then, we evaluated whether GDNF treatment could enhance the surface expression of receptors known to be involved in cell mobilization and engraftment within damaged tissues [32–34]. Flow cytometry histograms showed that hAFS cells constitutively expressed CD44, CXCR4, and CX3CR1 receptors, which were markedly enhanced by GDNF treatment (Fig. 7C).

Next, the effect of GDNF on hydrogen peroxide–induced cytotoxicity in hAFS cells was investigated. Hydrogen peroxide (200 μM for 24 h) significantly reduced hAFS cell viability in respect to untreated cells (45.8%±2% vs. 95.2%±0.7%, $P < 0.05$). GDNF markedly ($P < 0.05$) decreased hAFS cell susceptibility to hydrogen peroxide (72.9%±5.7%).

Human AFS cell production of proregenerative factors

The potential of hAFS cells to create a proregenerative microenvironment was investigated by studying hAFS cell production of factors with mitogenic and prosurvival action. The effect of GDNF treatment was also investigated. By multianalyte profiling assay, we observed that hAFS cells released in 48 h conditioned medium considerable amounts of IL-6, VEGF, SDF-1, and IGF-1 (350.3±16.8, 369.2±4.6, 469.3±10.1, and 61±1 pg/mL/10^6 cells, respectively). The levels of IL-10, FGF-2, and HGF were below the detection limits. When hAFS cells were exposed to GDNF, a markedly increased production of IL-6, VEGF, and SDF-1 was detected (416.4±5.5, 493.7±19.8, and 618.7±31.8 pg/ mL/10^6 cells). At variance IGF-1 secreted by GDNF-preconditioned cells was not increased (67±7 pg/mL/10^6 cells). The percentage of IL-6, VEGF, and SDF-1 production by GDNF-treated hAFS cells, compared with untreated cells, is shown in Fig. 7D.

Discussion

The recent discovery of a population of multipotent stem cells from human amniotic fluid exhibiting remarkable plasticity, high expansion potential, and a low risk for tumor development [22–24] has raised interest in studying the
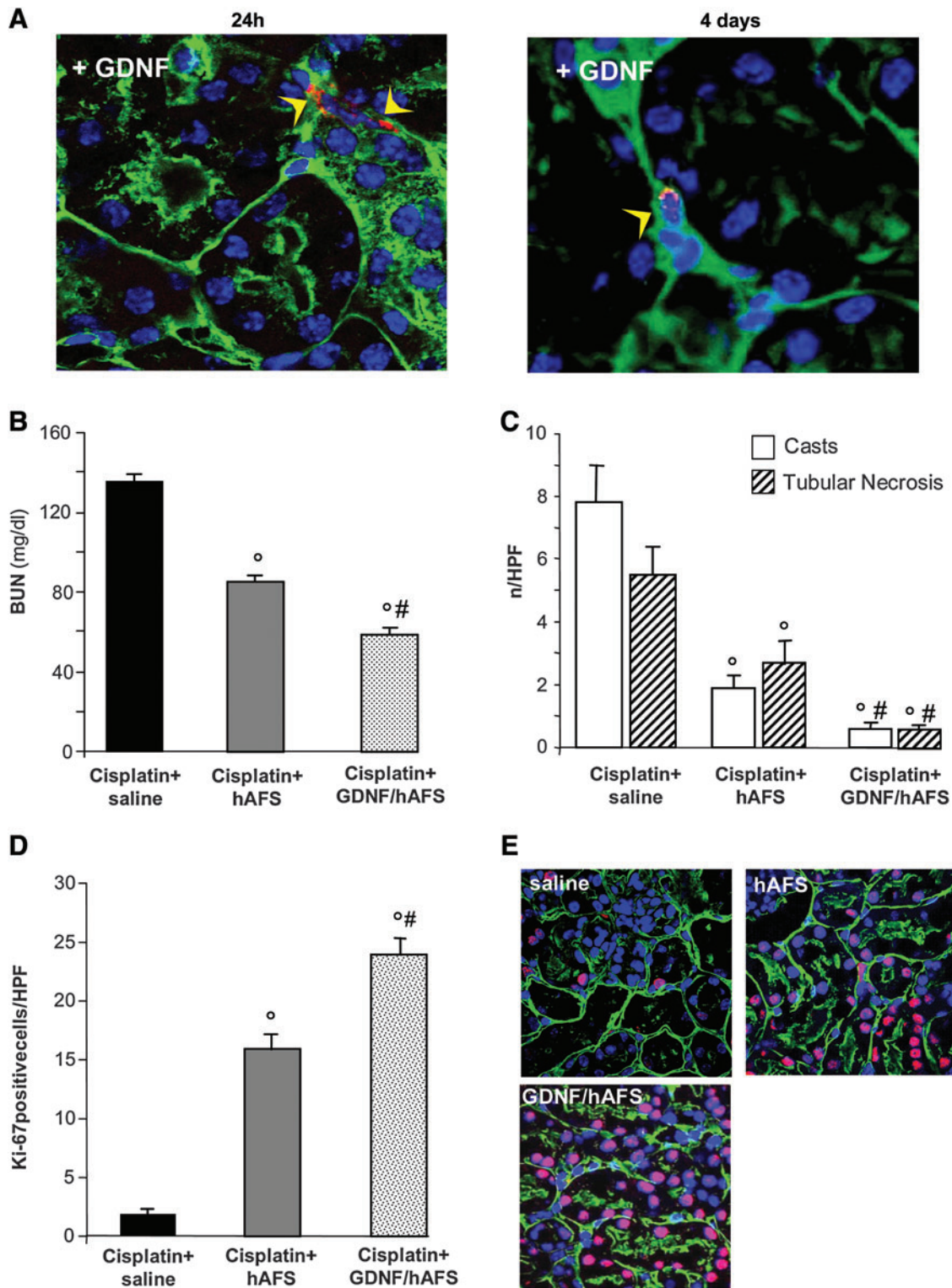
FIG. 6. Preconditioning with GDNF increases renoprotection of hAFS cells in mice with AKI. **(A)** Representative micrographs of renal tissue after 24 h (*left*) and at 4 days (*right*) from cisplatin-treated mice injected with hAFS PKH-26+ cells (*red*) preconditioned with GDNF (100 ng/mL for 24 h). Preconditioned hAFS PKH-26+ cells were localized in peritubular area (*arrow heads*). Original magnification 630×. The sections were stained with FITC-labeled lectin WGA (*green*), and DAPI for nuclei (*blue*). **(B)** Renal function, measured as BUN, in cisplatin-treated mice given saline, untreated hAFS cells or GDNF-preconditioned hAFS cells at 4 days. Data are mean±SE. °$P < 0.01$ versus cisplatin+saline; #$P < 0.05$ versus cisplatin+hAFS cells. **(C)** Histological changes in kidneys from cisplatin-treated mice receiving saline, untreated hAFS cells, or GDNF-preconditoned hAFS cells at 4 days. Data are mean±SE. °$P < 0.01$ versus cisplatin+saline; #$P < 0.01$ versus cisplatin+hAFS cells. **(D)** Quantification of Ki-67–positive tubular cells at 4 days after cisplatin treatment. Data are mean±SE. °$P < 0.01$ versus cisplatin+saline; #$P < 0.01$ versus cisplatin+hAFS cells. **(E)** Representative images of Ki-67–positive tubular cells (*red*) costained with FITC-labeled lectin WGA (*green*) and DAPI (*blue*) in kidney sections of cisplatin mice given saline, untreated hAFS cells, or GDNF-preconditioned hAFS cells. Original magnification 630×. GDNF, glial cell line–derived neurotrophic factor. Color images available online at www.liebertonline.com/scd

TABLE 5. COMPARISON BETWEEN HUMAN AMNIOTIC
FLUID STEM CELLS AND HUMAN BONE MARROW
MESENCHYMAL STEM CELLS ON SURVIVAL
OF CISPLATIN MICE WITH ACUTE KIDNEY INJURY

	Survival (%)			
	0 day	5 days	7 days	31 days
Cisplatin + saline	100	50	0	0
Cisplatin + hAFS	100	100	50	33[a]
Cisplatin + hBM-MSCs	100	83	33	33[a]

[a]$p < 0.009$ versus cisplatin + saline (Kaplan-Meier analysis and Log-Rank test).

hBM-MSCs, human bone marrow mesenchymal stem cells.

regenerative effect of this cell population in heart and lung diseases and neurological disorders [22,24,26]. In the current article, we tested whether hAFS cells induced a regenerative process in the kidney up to prolong animal survival using a model of cisplatin-induced acute kidney injury characterized by high mortality. Recent evidence documented the efficacy of intraparenchymally injected hAFS cells in preventing renal damage in nu/nu mice with glycerol-induced AKI when stem cells were given before the onset of renal damage [35]. Furthermore, renal regeneration by hAFS cells given at the time of overt disease in the same experimental model was recently reported, the protection being comparable with that of BM-MSCs [36]. However, in both studies no data on animal survival were provided. Here, we have documented in NOD/SCID mice with established cisplatin-induced AKI that hAFS cell treatment ameliorated tubular damage, limited renal function impairment, and prolonged animal lifespan. The favorable effect on survival was comparable with that of human BM-MSCs but lower than that previously reported for human CB-MSCs [15].

Another relevant information provided by the current article rests on data that hAFS cells accelerated the renal recovery in mice with AKI through a differentiation-independent mechanism. Upon infusion, hAFS cells specifically engrafted the damaged kidney—but not the other organs such as liver, heart, spleen, and lung—and predominantly localized in peritubular compartment rather than within the tubular epithelium, without differentiating in renal cells. This result is in contrast with the capacity of hAFS cells to acquire a renal phenotype when injected into primordial rodent kidney structures [27]. Moreover, when hAFS cells were infused into damaged renal parenchyma of adult mice with AKI, their renal differentiation capacity was modest [35]. These observations would suggest that only an embryonic microenvironment is able to create the appropriate condition for driving hAFS cells toward renal commitment.

The regenerative effect of hAFS cells on damaged kidney was mediated through a local paracrine action likely accomplished by the secretion of cytokines and growth factors with mitogenic and prosurvival effects [17,37,38] including IL-6, VEGF, SDF-1, and IGF-1 that were found in the conditioned medium of hAFS cells.

Renal toxicity of cisplatin manifests as increased tubular oxidative damage responsible for cell apoptosis and reduced phosphorylation of the prosurvival factor Akt [15], a key mediator of the phosphoinositide-3 kinase (PI3K) survival and mitogenic signals [30,31]. Blockade of PI3K-Akt pathway markedly accelerated tubular cell apoptosis and necrosis leading to a worse prognosis of cisplatin-treated mice [39]. Here, we have documented that treatment with hAFS cells exerted a local action by inhibiting tubular cell apoptosis in respect to cisplatin mice given saline. The capability of hAFS cells to create a regenerative environment was supported by the increased tubular expression of pAkt and proliferation at 4 days, the time point at which untreated mice exhibited higher tubular injury and apoptosis. These results indicate that local activation of renal intracellular signaling by hAFS cells elicits antiapoptotic and proliferative responses, a mechanism also operated by MSCs of BM and CB origin [14,15].

The current study also explored an additional way to maximize hAFS cell regenerative potential by preconditioning of cells before their in vivo injection. Data are already available that gene modification [40,41] or stem cell preconditioning with growth factors, cytokines, hypoxia, or other factors [28,42–44] can optimize in vitro and in vivo stem cell migration, engraftment, survival, and efficacy. Here, we focused on GDNF, a growth factor known to participate to early nephrogenesis [45], to induce adult stem cells toward renal commitment [46], and to improve motility and survival of stem cells in response to hypoxic stress condition [28]. GDNF increased stem cell migration and homing of hAFS cells in damaged kidney and reduced their susceptibility to the hypoxic environment, as reflected by the high number of GDNF-treated hAFS cells engrafting the renal tissue at 24 h that was also stably detectable at 4 days. However, GDNF exposure did not commit hAFS cells toward renal phenotype, as supported by cell engraftment limited to the peritubular site. The combined effect of preconditioning on hAFS cell engraftment and survival in injured tissue was associated with further amelioration of renal function, tubular injury, and proliferation. These data indicate that GDNF increases the tropism of hAFS cells for damaged tissue and further enhances the ability of these cells to locally promote repair. Consistent with in vivo data, GDNF enhanced the motility of cultured hAFS cells, upregulated the expression of surface receptors involved in chemotaxis and homing, and enhanced hAFS cell therapeutic potential by increasing the constitutive production of mitogenic and angiogenic factors. Moreover, enhanced survival of GDNF-treated hAFS cells, in response to a toxic concentration of hydrogen peroxide, suggests that GDNF can activate stem cell cytoprotective and antioxidant pathways capable to protect hAFS cells from oxidative stress occurring in damaged tissue.

In conclusion, this study suggests that hAFS cells represent a new potential stem cell source for organ regeneration at least to the extent that what we have seen in AKI may be applicable to other diseases. Mechanisms underlying tissue repair by hAFS cells operate through local activation of paracrine signals rather than cell differentiation. A new approach to enhance hAFS cell tropism and survival in damaged tissue has been proposed by preconditioning of stem cells with GDNF before their in vivo use.
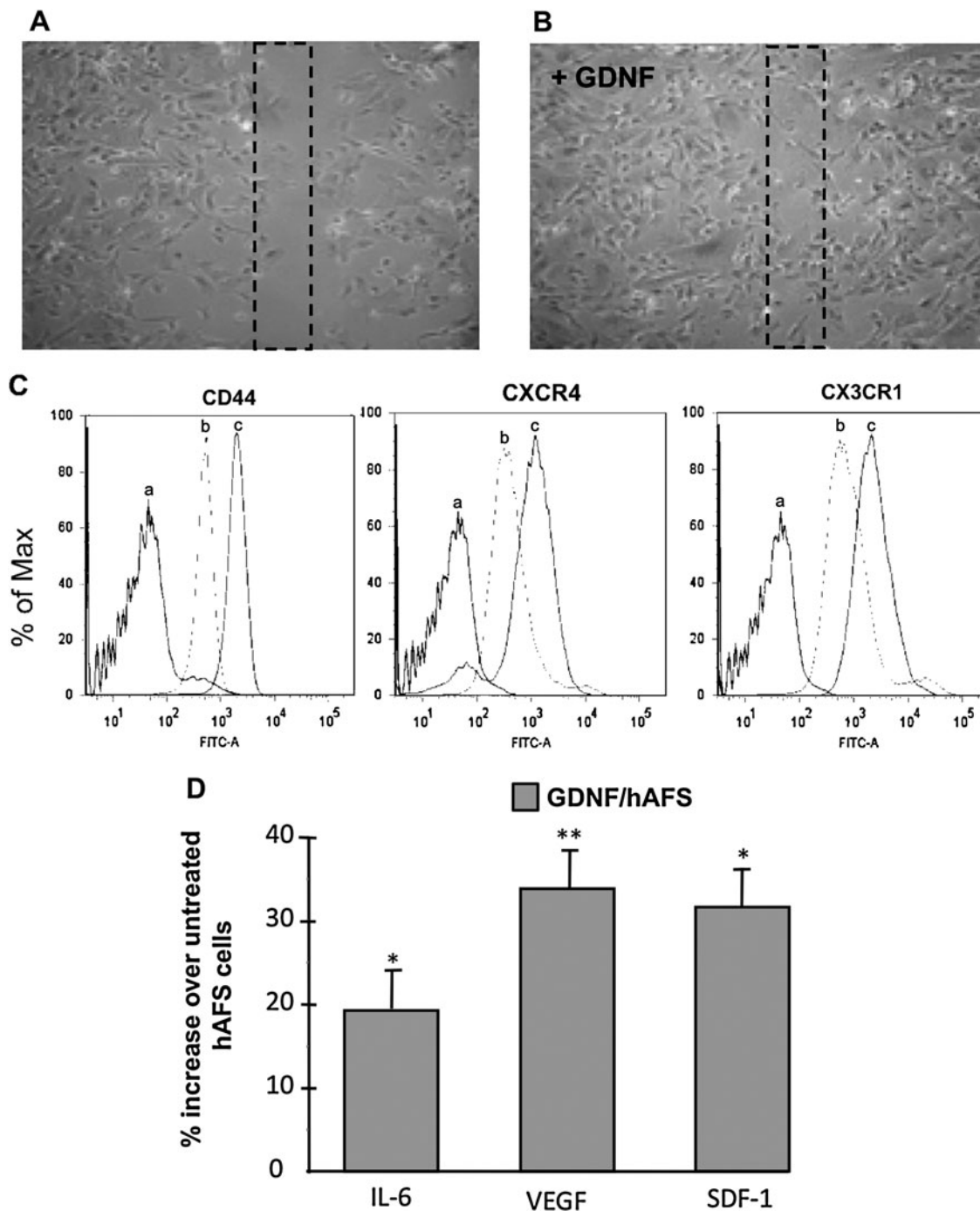
Acknowledgments

FIG. 7. GDNF increases in vitro hAFS cell motility; expression of CD44, CXCR4, and CX3CR1 receptors; and production of proregenerative factors. Representative micrographs of scratch-wound-closure assays in hAFS cells untreated **(A)** or treated for 24 h with GDNF (100 ng/mL) **(B)**. Preconditioned hAFS cells with GDNF showed a more rapid capacity to cover the wound area after 7 h in respect to untreated hAFS cells. **(C)** Representative fluorescence histograms show the expression of CD44, CXCR4, and CX3CR1 in untreated hAFS cells **(b)** and GDNF-conditioned hAFS cells **(c)** by FACs. The negative controls are shown **(a)**. **(D)** Effect of GDNF on cytokines/growth factors production by hAFS cells. Percentage of increased production of IL-6, VEGF, and SDF-1 by hAFS cells treated with GDNF (GDNF/hAFS) for 48 h in respect to untreated hAFS cells. $*P < 0.05$ and $**P < 0.01$ versus untreated hAFS cells. SDF, stromal cell–derived factor.

Author Disclosure Statement

No competing financial interests exist.

References

1. Choi YH, T Saric, B Nasseri, S Huhn, S Van Linthout, R Hetzer, C Tschope and C Stamm. (2011). Cardiac cell therapies: the next generation. Cardiovasc Ther 29:2–16.

2. Shimada IS and JL Spees. (2011). Stem and progenitor cells for neurological repair: minor issues, major hurdles, and exciting opportunities for paracrine-based therapeutics. J Cell Biochem 112:374–380.

3. Morigi M, A Benigni, G Remuzzi and B Imberti. (2006). The regenerative potential of stem cells in acute renal failure. Cell Transplant 15 (Suppl. 1):S111–S117.

4. Bussolati B, C Tetta and G Camussi. (2008). Contribution of stem cells to kidney repair. Am J Nephrol 28:813–822.

5. Mazzinghi B, E Ronconi, E Lazzeri, C Sagrinati, L Ballerini, ML Angelotti, E Parente, R Mancina, GS Netti, et al. (2008). Essential but differential role for CXCR4 and CXCR7 in the therapeutic homing of human renal progenitor cells. J Exp Med 205:479–490.

6. Hopkins C, J Li, F Rae and MH Little. (2009). Stem cell options for kidney disease. J Pathol 217:265–281.

7. Cheng Z, L Ou, X Zhou, F Li, X Jia, Y Zhang, X Liu, Y Li, CA Ward, LG Melo and D Kong. (2008). Targeted migration of mesenchymal stem cells modified with CXCR4 gene to infarcted myocardium improves cardiac performance. Mol Ther 16:571–579.

8. Iwatani H and E Imai. (2010). Kidney repair using stem cells: myth or reality as a therapeutic option? J Nephrol 23:143–146.

9. Herrera MB, B Bussolati, S Bruno, V Fonsato, GM Romanazzi and G Camussi. (2004). Mesenchymal stem cells contribute to the renal repair of acute tubular epithelial injury. Int J Mol Med 14:1035–1041.

10. Morigi M, B Imberti, C Zoja, D Corna, S Tomasoni, M Abbate, D Rottoli, S Angioletti, A Benigni, et al. (2004). Mesenchymal stem cells are renotropic, helping to repair the kidney and improve function in acute renal failure. J Am Soc Nephrol 15:1794–1804.

11. Togel F, Z Hu, K Weiss, J Isaac, C Lange and C Westenfelder. (2005). Administered mesenchymal stem cells protect against ischemic acute renal failure through differentiation-independent mechanisms. Am J Physiol Renal Physiol 289:F31–F42.

12. Bi B, R Schmitt, M Israilova, H Nishio and LG Cantley. (2007). Stromal cells protect against acute tubular injury via an endocrine effect. J Am Soc Nephrol 18:2486–2496.

13. Togel F, K Weiss, Y Yang, Z Hu, P Zhang and C Westenfelder. (2007). Vasculotropic, paracrine actions of infused mesenchymal stem cells are important to the recovery from acute kidney injury. Am J Physiol Renal Physiol 292:F1626-1635.

14. Morigi M, M Introna, B Imberti, D Corna, M Abbate, C Rota, D Rottoli, A Benigni, N Perico, et al. (2008). Human bone marrow mesenchymal stem cells accelerate recovery of acute renal injury and prolong survival in mice. Stem Cells 26:2075–2082.

15. Morigi M, C Rota, T Montemurro, E Montelatici, V Lo Cicero, B Imberti, M Abbate, C Zoja, P Cassis, et al. (2010). Life-sparing effect of human cord blood-mesenchymal stem cells in experimental acute kidney injury. Stem Cells 28:513–522.

16. Poulsom R, SJ Forbes, K Hodivala-Dilke, E Ryan, S Wyles, S Navaratnarasah, R Jeffery, T Hunt, M Alison, et al. (2001). Bone marrow contributes to renal parenchymal turnover and regeneration. J Pathol 195:229–235.

17. Imberti B, M Morigi, S Tomasoni, C Rota, D Corna, L Longaretti, D Rottoli, F Valsecchi, A Benigni, et al. (2007). Insulin-like growth factor-1 sustains stem cell mediated renal repair. J Am Soc Nephrol 18:2921–2928.

18. Duffield JS, KM Park, LL Hsiao, VR Kelley, DT Scadden, T Ichimura and JV Bonventre. (2005). Restoration of tubular epithelial cells during repair of the postischemic kidney occurs independently of bone marrow-derived stem cells. J Clin Invest 115:1743–1755.

19. Hyun I. (2010). The bioethics of stem cell research and therapy. J Clin Invest 120:71–75.

20. Odorico JS, DS Kaufman and JA Thomson. (2001). Multi-lineage differentiation from human embryonic stem cell lines. Stem Cells 19:193–204.

21. Takahashi K and S Yamanaka. (2006). Induction of pluripotent stem cells from mouse embryonic and adult fibroblast cultures by defined factors. Cell 126:663–676.

22. De Coppi P, G Bartsch, Jr., MM Siddiqui, T Xu, CC Santos, L Perin, G Mostoslavsky, AC Serre, EY Snyder, et al. (2007). Isolation of amniotic stem cell lines with potential for therapy. Nat Biotechnol 25:100–106.

23. Cananzi M, A Atala and P De Coppi. (2009). Stem cells derived from amniotic fluid: new potentials in regenerative medicine. Reprod Biomed Online 18 Suppl 1:17–27.

24. Carraro G, L Perin, S Sedrakyan, S Giuliani, C Tiozzo, J Lee, G Turcatel, SP De Langhe, B Driscoll, et al. (2008). Human amniotic fluid stem cells can integrate and differentiate into epithelial lung lineages. Stem Cells 26:2902–2911.

25. Ditadi A, P de Coppi, O Picone, L Gautreau, R Smati, E Six, D Bonhomme, S Ezine, R Frydman, M Cavazzana-Calvo and I Andre-Schmutz. (2009). Human and murine amniotic fluid c-Kit+Lin- cells display hematopoietic activity. Blood 113:3953–3960.

26. Tsuji H, S Miyoshi, Y Ikegami, N Hida, H Asada, I Togashi, J Suzuki, M Satake, H Nakamizo, et al. (2010). Xenografted human amniotic membrane-derived mesenchymal stem cells are immunologically tolerated and transdifferentiated into cardiomyocytes. Circ Res 106:1613–1623.

27. Perin L, S Giuliani, D Jin, S Sedrakyan, G Carraro, R Habibian, D Warburton, A Atala and RE De Filippo. (2007). Renal differentiation of amniotic fluid stem cells. Cell Prolif 40:936–948.

28. Shi H, D Patschan, GP Dietz, M Bahr, M Plotkin and MS Goligorsky. (2008). Glial cell line-derived neurotrophic growth factor increases motility and survival of cultured mesenchymal stem cells and ameliorates acute kidney injury. Am J Physiol Renal Physiol 294:F229–F235.

29. Bonegio R and W Lieberthal. (2002). Role of apoptosis in the pathogenesis of acute renal failure. Curr Opin Nephrol Hypertens 11:301–308.

30. Datta SR, A Brunet and ME Greenberg. (1999). Cellular survival: a play in three Akts. Genes Dev 13:2905–2927.

31. Chang F, JT Lee, PM Navolanic, LS Steelman, JG Shelton, WL Blalock, RA Franklin and JA McCubrey. (2003). Involvement of PI3K/Akt pathway in cell cycle progression, apoptosis, and neoplastic transformation: a target for cancer chemotherapy. Leukemia 17:590–603.

32. Herrera MB, B Bussolati, S Bruno, L Morando, G Mauriello-Romanazzi, F Sanavio, I Stamenkovic, L Biancone and G Camussi. (2007). Exogenous mesenchymal stem cells localize

to the kidney by means of CD44 following acute tubular injury. Kidney Int 72:430–441.

33. Shi M, J Li, L Liao, B Chen, B Li, L Chen, H Jia and RC Zhao. (2007). Regulation of CXCR4 expression in human mesenchymal stem cells by cytokine treatment: role in homing efficiency in NOD/SCID mice. Haematologica 92:897–904.

34. Ji JF, BP He, ST Dheen and SS Tay. (2004). Interactions of chemokines and chemokine receptors mediate the migration of mesenchymal stem cells to the impaired site in the brain after hypoglossal nerve injury. Stem Cells 22:415–427.

35. Perin L, S Sedrakyan, S Giuliani, S Da Sacco, G Carraro, L Shiri, KV Lemley, M Rosol, S Wu, et al. (2010). Protective effect of human amniotic fluid stem cells in an immunodeficient mouse model of acute tubular necrosis. PLoS One 5:e9357.

36. Hauser PV, R De Fazio, S Bruno, S Sdei, C Grange, B Bussolati, C Benedetto and G Camussi. (2010). Stem cells derived from human amniotic fluid contribute to acute kidney injury recovery. Am J Pathol 177:2011–2021.

37. Waxman AB and N Kolliputi. (2009). IL-6 protects against hyperoxia-induced mitochondrial damage via Bcl-2-induced Bak interactions with mitofusins. Am J Respir Cell Mol Biol 41:385–396.

38. Neufeld G, T Cohen, S Gengrinovitch and Z Poltorak. (1999). Vascular endothelial growth factor (VEGF) and its receptors. FASEB J 13:9–22.

39. Kuwana H, Y Terada, T Kobayashi, T Okado, JM Penninger, J Irie-Sasaki, T Sasaki and S Sasaki. (2008). The phosphoinositide-3 kinase gamma-Akt pathway mediates renal tubular injury in cisplatin nephrotoxicity. Kidney Int 73:430–445.

40. Hagiwara M, B Shen, L Chao and J Chao. (2008). Kallikrein-modified mesenchymal stem cell implantation provides enhanced protection against acute ischemic kidney injury by inhibiting apoptosis and inflammation. Hum Gene Ther 19:807–819.

41. Mangi AA, N Noiseux, D Kong, H He, M Rezvani, JS Ingwall and VJ Dzau. (2003). Mesenchymal stem cells modified with Akt prevent remodeling and restore performance of infarcted hearts. Nat Med 9:1195–1201.

42. Mias C, E Trouche, MH Seguelas, F Calcagno, F Dignat-George, F Sabatier, MD Piercecchi-Marti, L Daniel, P Bianchi, et al. (2008). *Ex vivo* pretreatment with melatonin improves survival, proangiogenic/mitogenic activity, and efficiency of mesenchymal stem cells injected into ischemic kidney. Stem Cells 26:1749–1757.

43. Schmidt A, D Ladage, T Schinkothe, U Klausmann, C Ulrichs, FJ Klinz, K Brixius, S Arnhold, B Desai, et al. (2006). Basic fibroblast growth factor controls migration in human mesenchymal stem cells. Stem Cells 24:1750–1758.

44. Hung SC, RR Pochampally, SC Hsu, C Sanchez, SC Chen, J Spees and DJ Prockop. (2007). Short-term exposure of multipotent stromal cells to low oxygen increases their expression of CX3CR1 and CXCR4 and their engraftment *in vivo*. PLoS One 2:e416.

45. Costantini F and R Shakya. (2006). GDNF/Ret signaling and the development of the kidney. Bioessays 28:117–127.

46. Yokoo T, T Ohashi, JS Shen, K Sakurai, Y Miyazaki, Y Utsunomiya, M Takahashi, Y Terada, Y Eto, T Kawamura, N Osumi and T Hosoya. (2005). Human mesenchymal stem cells in rodent whole-embryo culture are reprogrammed to contribute to kidney tissues. Proc Natl Acad Sci U S A 102:3296–3300.

Address correspondence to:
Dr. Marina Morigi
"Mario Negri" Institute for Pharmacological Research
Centro Anna Maria Astori
Science and Technology Park Kilometro Rosso
Via Stezzano, 87
Bergamo 24126
Italy

E-mail: marina.morigi@marionegri.it